ELSEVIER

International Journal of Mass Spectrometry 202 (2000) 37–45

International Journal of Mass Spectrometry

Ion/molecule reactions of *o*-carborane(12) and a method for identifying overlapped isotopic distributions in complex mass spectra

Fiona H. Scholes[a], Richard J.S. Morrison[a,*], Colin L. Raston[a], Gary H. Kruppa[b]

[a]*Department of Chemistry, Monash University, PO Box 23, Victoria, 3800, Australia*
[b]*Bruker Daltonics, Manning Park, Billerica, MA 01821, USA*

Received 2 April 1999; accepted 16 February 2000

Abstract

A high resolution Fourier transform ion cyclotron resonance mass spectrometer was used to investigate gas phase ion/molecule reactions of *o*-carborane(12) (*o*-$C_2B_{10}H_{12}$). The reaction of *o*-carborane(12) neutrals and cations produced oligomeric carborane species. Extensive hydrogen losses and H_2O/CH_3OH adducts were also observed and these resulted in complex mass spectra containing overlapped isotopic distributions. For a cell pressure of 6.0×10^{-9} mbar and for reaction delays from 50 ms to 30 s, some 73 species were identified in the resultant mass spectra, and their reaction kinetics were explored using a simplified, six step reaction mechanism. The analysis of these complex mass spectra was simplified by MACLOOMIS, an interactive program based on pattern recognition techniques originally developed for the analysis of high resolution vibration–rotation spectra. When adapted to mass spectra, MACLOOMIS enabled the rapid identification of overlapped isotopic distributions, and this approach may prove useful for a wide range of mass spectrometry studies. (Int J Mass Spectrom 202 (2000) 37–45) © 2000 Elsevier Science B.V.

Keywords: Carborane; FT/ICR-MS; Ion–molecule reactions; Spectral deconvolution

1. Introduction

The Fourier transform ion cyclotron resonance (FTICR) mass spectrometer has been used extensively for studying gas phase ion/molecule reactions. This particular application was demonstrated early in ICR development [1] and has been the subject of several review articles [2–4]. The instrument couples ion trapping techniques with ultrahigh resolving powers, making it ideal for studying complex ion/molecule reaction systems. Reported herein are the results concerning the complex *o*-$C_2B_{10}H_{12}$ [1,2-dicarba-*closo*-dodecaborane(12) or *o*-carborane(12)] system, together with a method for identifying overlapped isotopic distributions in the mass spectra obtained.

o-$C_2B_{10}H_{12}$ is shown in Fig. 1. This electron-deficient cage compound is stable at temperatures in excess of 400 °C, and has been incorporated into polymeric chains to produce polymers with high thermal stability [5,6]. Such polymers have comprised *o*-$C_2B_{10}H_{12}$ cages linked indirectly by a range of interstitial groups. In contrast, however, a variety of directly linked carborane oligomers have also been

* Author to whom correspondence should be addressed.

PII S1387-3806(00)00231-1

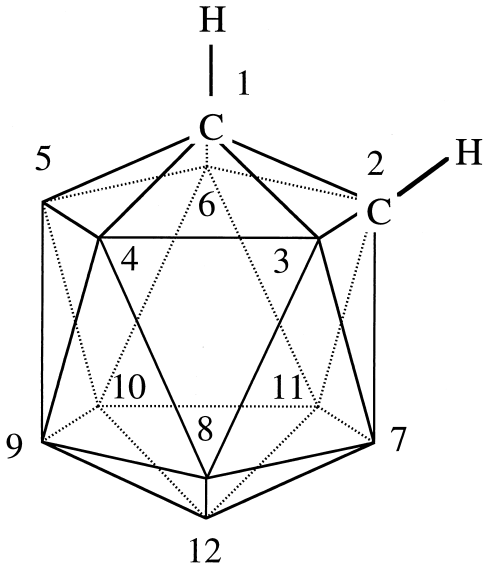

Fig. 1. 1,2-dicarba-*closo*-dodecaborane(12) or *o*-carborane(12). Vertices are numbered according to IUPAC conventions and unmarked vertices = BH.

produced. Shortly after the initial discovery of *o*-$C_2B_{10}H_{12}$ and the *m*- and *p*-isomers [7–10], the preparation of 1,1′-bis[*o*-carborane(12)] was reported [11]. More recent reports have described carborane oligomers up to four cages in length produced by the Cu(II)-mediated coupling reaction of the dilithiated salt of *p*-$C_2B_{10}H_{12}$ [12,13]. Similar synthetic methods have also produced the dimeric species 1,3′-bis[*o*-carborane(12)], 1,4′-bis[*o*-carborane(12)], and 1,1′-bis[*m*-carborane(12)] and the tetrameric tetra[*m*-carborane(12)] [14]. These four species involve C–B, C–B, C–C, and C–C bonds, respectively, between interconnected carborane cages. Alternative synthetic routes have produced two B–B linked dimers [15,16] and a cyclic trimer has been produced in low yield by γ-irradiation of *o*-$C_2B_{10}H_{12}$ [17].

The synthetic routes described above for producing carborane oligomers generally utilise the electron-deficient nature of the carboranes and thus involve anionic carborane intermediates. In the present study, the reactions between *o*-$C_2B_{10}H_{12}$ neutrals and the corresponding positively charged ions produced oligomeric carborane cations in which up to five *o*-$C_2B_{10}H_{12}$ cages are directly linked.

Carborane ions produce very complex mass spectra with broad isotopic distributions resulting from the two boron isotopes ^{10}B(19.78%) and ^{11}B(80.22%). Furthermore, previous mass spectrometry studies have shown that fragmentation is extensive and is mainly due to hydrogen losses [18,19], although dehydrogenation is suppressed in organometallic derivatives of some carboranes [20,21]. Both positive and negative ion spectra also exhibit the loss of borane units from the boron–carbon skeleton [18,19,22,23]. Given the high resolving power of the FTICR mass spectrometer, these factors lead to many closely spaced spectral peaks and overlapped isotopic distributions. The present article demonstrates the application of MACLOOMIS [24], a spectral line fitting program which largely simplified the analysis of these complex mass spectra.

MACLOOMIS is an interactive fitting program originally designed for the analysis of high resolution vibration–rotation spectra. It is based on the computer program developed by Winnewisser et al. [25] in which spectra are displayed on a computer screen as Loomis-Wood diagrams. The principle of the Loomis-Wood diagram [26] is to replot the spectrum in segments of width 2*B* where *B* is the rotational constant. Successive segments are displayed one above the other. Thus, any series of spectral lines spaced by 2*B* will appear as a vertical series which is easily identifiable by pattern recognition.

When adapted to an analysis of the mass spectra of carborane ions, the value specified for *B* is 0.4982 corresponding to a spacing 2*B* of 0.9964*m/z*. This is the spacing between isotopic peaks for singly charged carborane ions. Multiply charged ions can also be identified by changing the value of *B* to 0.2491 and 0.1667 for doubly and triply charged ions, respectively. Overlapped isotopic distributions are then easily identified as vertical series in the MACLOOMIS plot. Thus, MACLOOMIS becomes a powerful tool for the analysis of carborane spectra containing hundreds of peaks and overlapped isotopic distributions.

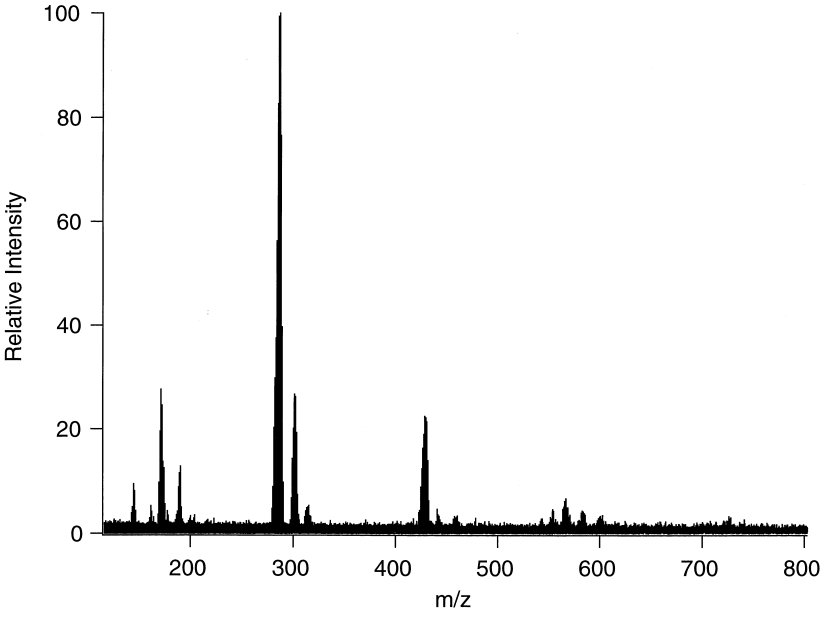

Fig. 2. The mass spectrum resulting from ion/molecule reactions at a cell pressure of 6.0×10^{-8} mbar and for a reaction delay of 30 s, demonstrating the formation of oligomeric carborane ions.

2. Experimental

A Bruker Daltonics APEX 47e FTICR mass spectrometer (Billerica, USA) with a magnetic field strength of 4.7 tesla was used in this study. A detailed description and the general operating procedures of this instrument have been reported previously [27].

o-$C_2B_{10}H_{12}$ (Aldrich) was admitted into the FTICR cell via a leak valve and the cell pressure was monitored by a Penning ionisation gauge. Ions were generated in the cell by internal electron ionisation with an electron energy of 70 eV, a filament current of 2.9 A and an ionisation pulse length of 20 ms. Positive ions were then trapped in the FTICR cell. The reaction delay prior to detection was varied from 50 ms to 60 s.

3. Results and discussion

The formation of oligomeric carborane ions is demonstrated in Fig. 2. This spectrum results from ion/molecule reactions at a cell pressure of 6.0×10^{-8} mbar and for a reaction delay of 30 s. Five distinct clusters of spectral peaks can be observed in the regions *m/z* 140–200, *m/z* 270–320, *m/z* 410–470, *m/z* 540–610, and *m/z* 700–750. For reaction delays longer than 30 s, peaks at higher *m/z* were not detected and the reaction appeared to reach equilibrium.

The isotopic distribution with highest relative abundance in Fig. 2 corresponds to the dimeric carborane ion ($C_4B_{20}H_{22}^{+\cdot}$ with base peak *m/z* 286) as confirmed by CID fragmentation studies. Oligomeric carborane ions as large as the pentameric species ($C_{10}B_{50}H_{52}^{+\cdot}$ with base peak *m/z* 714) can be seen in the spectrum. Additional isotopic distributions are also visible (e.g. in the region *m/z* 170–180) which cannot correspond to simple oligomeric carborane ions.

To simplify the analysis of these complex mass spectra, the task of identifying all species was restricted to spectra obtained at a cell pressure of 6.0×10^{-9} mbar. Under these conditions the reaction appeared to reach equilibrium after 30 s and no spectral peaks were observed beyond the dimeric region. The formation of trimeric and larger oligomers was negligible thereby producing more simple mass spectra. A representative spectrum is shown in Fig. 3.

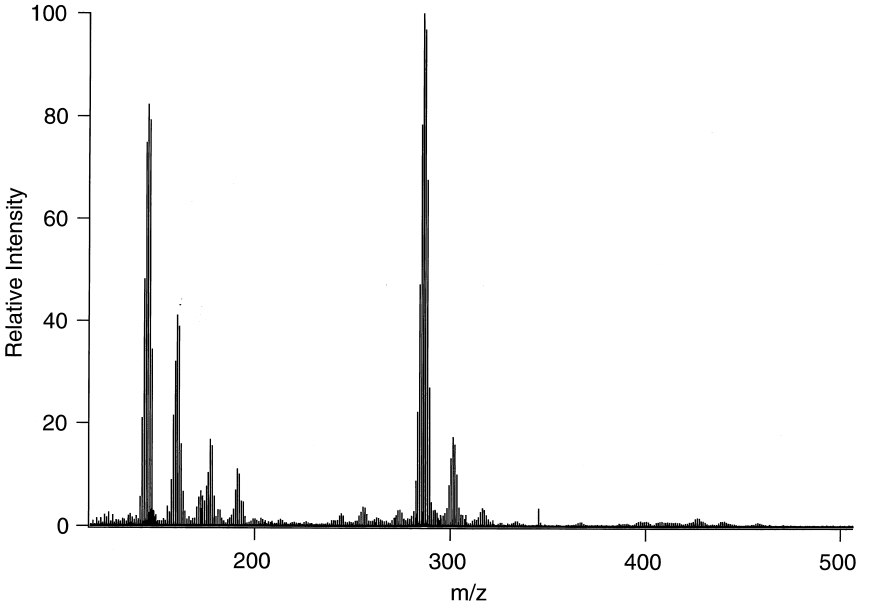

Fig. 3. The mass spectrum resulting from ion/molecule reactions at a cell pressure of 6.0×10^{-9} mbar and for a reaction delay of 30 s.

The identification of all species remained a difficult task because the spectra were further complicated by carborane ions undergoing multiple hydrogen losses. Consider the isotopic distribution for $C_2B_{10}H_{12}^{+\cdot}$ in which each peak is separated by 0.996 37 *m/z* units. When one hydrogen atom is removed to produce $C_2B_{10}H_{11}^{+}$ the isotopic distribution is shifted to lower *m/z* by 1.007 825 *m/z* units. Consequently, the two isotopic distributions overlap significantly and it is difficult to determine which spectral peaks correspond to each particular species. The complexity of these spectra is highlighted in Fig. 4. There are six closely spaced peaks with a nominal *m/z* of 133 each resulting from a different carborane species.

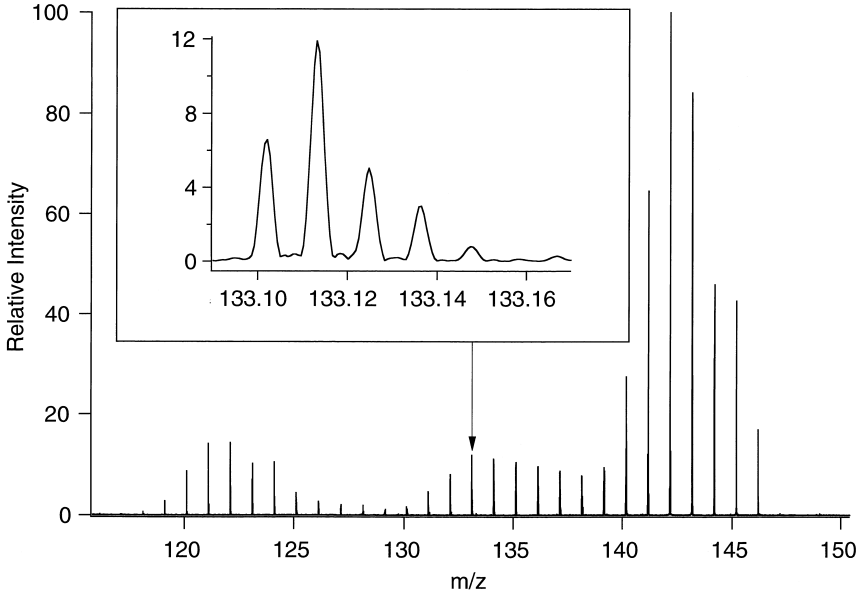

Fig. 4. The mass spectrum resulting from ion/molecule reactions at a cell pressure of 6.0×10^{-9} mbar and for a reaction delay of 50 ms. There are six closely spaced peaks with a nominal *m/z* of 133, each resulting from a different carborane ion.

Previously, a number of groups have described algorithms to automatically assign charge state and mass in complex electrospray ionisation mass spectra having resolved isotopic peaks. Spectral deconvolution using an entropy-based algorithm has been reported [28], while another approach is to perform a fourier transform on mass-domain data and then to identify mass spacings by the frequency spike(s) in the corresponding FT domain [29]. A technique combining the latter approach with the computation of Patterson charge maps has also been successfully demonstrated [29]. Zhang and Marshall [30] have described an algorithm (ZSCORE) that uses peak spacing information to determine the maximum possible charge state for a peak, then identifies the true charge state using a charge scoring system. Finally, isotopic family members are picked out by examining the spacings between peaks having the determined charge state; these peaks are then transformed into a so-called "zero-charge" mass spectrum.

In the present work we have adopted a new approach, borrowing a technique from molecular spectroscopy to greatly simplify the analysis of each mass spectrum. A computer program (MACLOOMIS) takes an expected peak spacing (e.g. 0.9964 Da—the successive isotope difference for carborane species whose boron content is $^{10}B_m{}^{11}B_n$—with various values for m and n) and displays a peak list in a graphical format that allows families of isotope peaks to be quickly recognized. In the mass spectra considered here there are many such families, corresponding to carborane ions having different numbers of hydrogen atoms. Each of these shows up on the MACLOOMIS plot as a distinct vertical series. Fig. 5 shows a portion of the MACLOOMIS plot for the mass spectrum obtained at a cell pressure of 6.0×10^{-9} mbar and for a reaction delay of 0.50 s. The value specified for B was 0.4982 corresponding to a spacing $2B$ of 0.9964m/z. As Fig. 5 shows, overlapping isotopic distributions are resolved and easily identified by pattern recognition.

The ions identified using MACLOOMIS are summarised in Table 1. Some 73 species were identified, or 17 if hydrogen losses are excluded. The monomeric species $C_2B_{10}H_x{}^{n+}$ was observed as singly, doubly, and triply charged ions ($n = 1, 2, 3$) and the dimeric species $C_4B_{20}H_x{}^{n+}$ was observed as singly and triply charged ions ($n = 1, 3$). Numerous fragment ions resulting from BH_x losses were also identified.

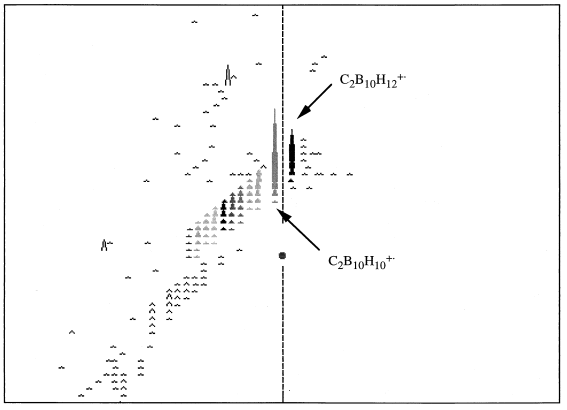

Fig. 5. MACLOOMIS output for the mass spectrum obtained at a cell pressure of 6.0×10^{-9} mbar and a reaction delay of 0.50 s. MACLOOMIS takes the peak list and displays the data in the form of a Loomis-Wood diagram in which the peak positions together with their amplitudes are represented in a two dimensional plane. Each marker on the diagram denotes a single spectral peak whose size denotes the peak's magnitude (divided into one of ten ranges). The data are then plotted in 57 strips arranged in rows, one above the next, with the first starting in the bottom left corner of the frame at a low mass of 109.306 Da, and the last finishing in the upper right corner of the frame at a high mass of 166.101 Da. To distinguish families of boron isotopes, each strip plots an interval of exactly 0.9964 Da, then wraps back to a new row starting at the left side of the frame, causing successive members of an isotopic series to appear as a series of markers lining up in a vertical group. The dark series shown just to the right of the cursor (the circle and dashed vertical line) corresponds to $C_2B_{10}H_{12}{}^{+\cdot}$ and the lighter series just to the left of the cursor results from $C_2B_{10}H_{10}{}^{+\cdot}$. Other series corresponding to $C_2B_{10}H_x^+$ for $x = 0$–8 can be clearly seen arranged in vertical columns looking further left and diagonally downwards in this diagram. Two intense peaks can also be seen which are due to residual calibrant ions (perfluorotributylamine).

Interestingly, several species containing oxygen and additional carbon atoms were identified and are thought to be adducts containing H_2O and/or CH_3OH. Given that H_2O/CH_3OH is a common electrospray solvent system, it is possible that the FTICR cell contained residual H_2O and CH_3OH from routine electrospray experiments on the instrument. These neutrals must have participated in ion/molecule reactions with the carborane ions thereby giving rise to the observed products.

Table 1
Summary of the species identified in mass spectra resulting from ion/molecule reactions with a cell pressure of 6.0×10^{-9} mbar and for reaction delays from 50 ms to 30 s. Letter codings (a)–(e) indicate the various groupings of ions used in the kinetic analysis.

$C_2B_{10}H_{13}^{3+}$	$C_2B_9H_{11}^{+\cdot}$	$C_2B_7H_3^{+\cdot}$	$C_2B_{10}H_7(OH_2)_3^{+}$ (c)
$C_2B_{10}H_{12}^{3+\cdot}$	$C_2B_9H_{10}^{+}$	$C_2B_7H_2^{+}$	$C_2B_{10}H_5(OH_2)_3^{+}$ (c)
$C_2B_{10}H_{11}^{3+}$	$C_2B_9H_9^{+\cdot}$	$C_2B_7H^{+\cdot}$	
$C_2B_{10}H_{10}^{3+\cdot}$	$C_2B_9H_8^{+}$	$C_2B_7^{+}$	$C_2B_{10}H_{10}OH_2^{3+}$
$C_2B_{10}H_8^{3+\cdot}$	$C_2B_9H_7^{+\cdot}$		$C_2B_{10}H_9OH_2^{3+}$
	$C_2B_9H_6^{+}$	$C_2B_6H_2^{+\cdot}$	$C_2B_{10}H_8OH_2^{3+}$
$C_2B_{10}H_{10}^{2+}$	$C_2B_9H_5^{+\cdot}$	$C_2B_6H^{+}$	
$C_2B_{10}H_8^{2+}$	$C_2B_9H_4^{+}$	$C_2B_6^{+\cdot}$	$C_4B_{20}H_{22}^{+\cdot}$ (d)
$C_2B_{10}H_6^{2+}$	$C_2B_9H_3^{+\cdot}$		$C_4B_{20}H_{18}^{+\cdot}$ (d)
$C_2B_{10}H_4^{2+}$	$C_2B_9H_2^{+}$	$C_2B_{10}H_{11}OH_2^{+}$ (c)	$C_4B_{20}H_{15}^{+}$ (d)
	$C_2B_9H^{+\cdot}$	$C_2B_{10}H_{10}OH_2^{+\cdot}$ (c)	
$C_2B_{10}H_{13}^{+}$ (b)	$C_2B_9^{+}$	$C_2B_{10}H_9OH_2^{+}$ (c)	$C_4B_{20}H_{19}OH_2^{+}$ (e)
$C_2B_{10}H_{12}^{+\cdot}$ (a)		$C_2B_{10}H_8OH_2^{+\cdot}$ (c)	
$C_2B_{10}H_{11}^{+}$ (b)	$C_2B_8H_8^{+\cdot}$		$C_4B_{20}H_{22}^{3+\cdot}$
$C_2B_{10}H_{10}^{+\cdot}$ (a)	$C_2B_8H_7^{+}$	$C_2B_{10}H_{11}CH_3OH^{+}$ (c)	
$C_2B_{10}H_9^{+}$ (a)	$C_2B_8H_6^{+\cdot}$	$C_2B_{10}H_9CH_3OH^{+}$ (c)	
$C_2B_{10}H_8^{+\cdot}$ (a)	$C_2B_8H_5^{+}$	$C_2B_{10}H_7CH_3OH^{+}$ (c)	
$C_2B_{10}H^{7+}$ (a)	$C_2B_8H_4^{+\cdot}$		
$C_2B_{10}H_6^{+\cdot}$ (a)	$C_2B_8H_3^{+}$	$C_2B_{10}H_7(CH_3OH)(OH_2)^{+}$ (c)	
$C_2B_{10}H_5^{+}$ (a)	$C_2B_8H_2^{+\cdot}$	$C_2B_{10}H_5(CH_3OH)(OH_2)^{+}$ (c)	
$C_2B_{10}H_4^{+\cdot}$ (a)	$C_2B_8H^{+}$		
$C_2B_{10}H_3^{+}$ (a)	$C_2B_8^{+\cdot}$	$C_2B_{10}H_7(CH_3OH)_2^{+}$ (c)	
$C_2B_{10}H_2^{+\cdot}$ (a)		$C_2B_{10}H_5(CH_3OH)_2^{+}$ (c)	
$C_2B_{10}H^{+}$ (a)			
$C_2B_{10}^{+\cdot}$ (a)		$C_2B_{10}H_9(OH_2)_2^{+}$ (c)	

The $C_2B_{10}H_{12}^{+\cdot}$ parent ion exhibits hydrogen losses resulting in the removal of up to 12 hydrogen atoms. External electron ionisation experiments confirmed that hydrogen losses resulted primarily from the electron ionisation process. However, hydrogen loss and transfer also occurred during the reaction period.

Once all the ions had been successfully identified using MACLOOMIS, the temporal evolution of the various signals was investigated. A series of mass spectra were recorded after reaction delays of 1, 2, 5, 10, and 20 s. Absolute intensities were obtained as a function of reaction time by summing the intensities of all isotopic peaks for each individual ion species. Monomeric carborane ions $C_2B_{10}H_x^+$ (x = 12, 10, 9, . . .) are initially the most abundant species while the formation of dimer ions and H_2O/CH_3OH adducts dominates for longer reaction delays. The ions $C_2B_{10}H_{11}^+$ and $C_2B_{10}H_{13}^+$ are interesting in that they show markedly different temporal profiles to the other $C_2B_{10}H_x^+$ species. Under the experimental conditions employed in this experiment, the abundance of both $C_2B_{10}H_{11}^+$ and $C_2B_{10}H_{13}^+$ ions rises initially from zero to reach a maximum at ~ 10 s, then decreases slowly at longer reaction times.

Due to the complexity of the reaction chemistry in this carborane system, we have chosen to organize the most abundant species into five groups, which have been coded with the letters (a)–(e) in Table 1. Group (a) consists of ions of general formula $C_2B_{10}H_x^+$ (x = 12, 10, 9, . . .). On the basis of their different time dependence, ions $C_2B_{10}H_x^+$ with x = 11, 13 are collected together in group (b). The remaining three groupings in this highly simplified picture of the reaction kinetics include water/methanol adducts of the monomer (c), dimeric species (d), and water/methanol adducts of the dimer (e).

The time evolution of the "lumped" signal from ions in each of these five groups is shown by the points marked by symbols in Fig. 6. Throughout the course of the reaction, multiply charged ions and fragment ions of the type $C_2B_9H_x^+$ and smaller are

present in low abundance and these species have been neglected in this process.

A simplified scheme which aims to describe the various reactions occurring at a cell pressure of 6×10^{-9} mbar is shown in the following.

For $x = 12, 10, 9, \ldots$:

$$C_2B_{10}H_{12} + C_2B_{10}H_x^+ \xrightarrow{k_1} C_4B_{20}H_y^+$$

$$[CH_3OH/H_2O] + C_2B_{10}H_x^+ \xrightarrow{k_2} C_2B_{10}H_a(OH_2)_b(CH_3OH)_c^+$$

$$C_2B_{10}H_{12} + C_2B_{10}H_a(OH_2)_b(CH_3OH)_c^+ \xrightarrow{k_3} C_4B_{20}H_d(OH_2)_b(CH_3OH)_c^+$$

For $x = 11, 13$:

$$[H] + C_2B_{10}H_x^+ \ (x \neq 11, 13) \xrightarrow{k_4} C_2B_{10}H_x^+$$

$$C_2B_{10}H_{12} + C_2B_{10}H_x^+ \xrightarrow{k_5} C_4B_{20}H_y^+$$

$$[CH_3OH/H_2O] + C_2B_{10}H_x^+ \xrightarrow{k_6} C_2B_{10}H_a(OH_2)_b(CH_3OH)_c^+$$

This scheme incorporates two distinct pools of monomer ions which may inter-convert, or undergo ion–molecule reactions with neutral *o*-$C_2B_{10}H_{12}$ or with solvent molecules such as water and/or methanol forming adduct species. The latter in turn may participate in further reactions with neutral *o*-$C_2B_{10}H_{12}$ giving rise to dimer adduct ions. [H] represents the numerous sources of hydrogen (both neutrals and ions).

The previous scheme was explored with a numerical modeling program [31]. The concentrations of *o*-$C_2B_{10}H_{12}$, [CH_3OH/H_2O], and [H] were assumed to be constant, giving five differential equations for five time-variable species and six pseudo-first-order rate constants (k_1–k_6). Initial estimates for k_1–k_6 were entered into the modeling program, which adjusted these constants to provide a least squares fit to the experimental data. The curves in Fig. 6 show the results of the fit. The fitted rate constants were found to be $k_1 = 0.023\ s^{-1}$, $k_2 = 0.020\ s^{-1}$, $k_3 = 0.018\ s^{-1}$, $k_4 = 0.084\ s^{-1}$, $k_5 = 0.0084\ s^{-1}$, and $k_6 = 0.091\ s^{-1}$.

The model predictions of ion relative abundance versus reaction delay shown in Fig. 6 are in quite reasonable agreement with the experimental data, particularly when one considers the crudeness of the trial kinetic model and the many assumptions inherent in grouping species together in the manner just described. Both experimental and calculated data sets show that the concentrations of monomeric carborane ions in each of the groups (a), (b), and (c) become equal after ~ 10 s, with $C_2B_{10}H_x^+$ ($x = 11, 13$) represented by group (b) reaching a plateau here before decreasing at longer reaction delays. The general shapes of the curves for the various monomeric carborane species are also quite similar in both model and experiment, although the adduct species (c) are slightly overpredicted in the model calculations beyond 15 s. Another obvious discrepancy is in the onset behavior for the dimer adducts $C_4B_{20}H_d(OH_2)_b(CH_3OH)_c^+$ [group (e)], which appear much earlier in the model calculations than in the experiment. Efforts to further refine the proposed

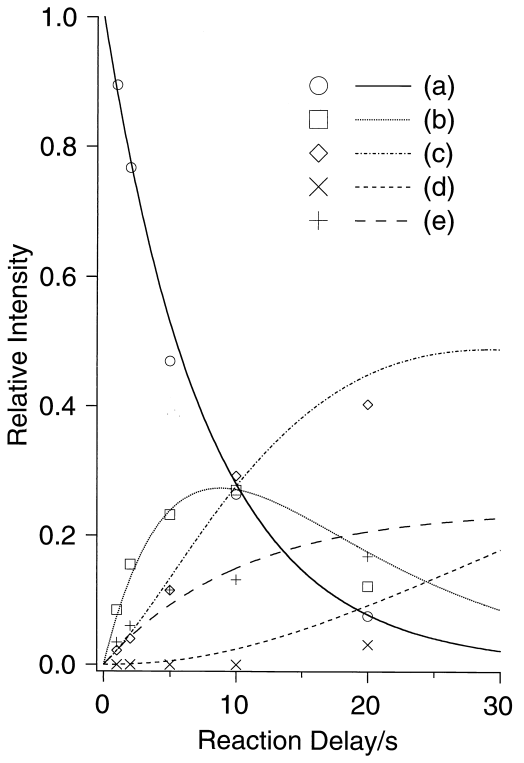

Fig. 6. Temporal evolution of ion signals at an ICR cell pressure of 6.0×10^{-9} mbar. For inclusion, ions have been grouped into five distinct categories labeled (a)–(e) as follows. Category (a) consists of ions of general formula $C_2B_{10}H_x^+$ (x = 12, 10, 9, . . .). On the basis of their different time dependence, ions $C_2B_{10}H_x^+$ with x = 11, 13 are collected together in category (b). The remaining three categories in this highly simplified picture of the reaction kinetics include water/methanol adducts of the monomer (c), dimeric species (d), and water/methanol adducts of the dimer (e). All members of an isotopic distribution are first summed together in order to produce the data shown. The points represent experimental data. The curves show the results of a least squares fit of the experimental points to a simplified kinetic model of the carborane reaction chemistry.

mechanism are probably of limited value given the complexity of the system under investigation.

4. Conclusions

It has been shown that ion/molecule reactions involving *o*-$C_2B_{10}H_{12}$ neutrals and cations produce oligomeric carborane species. Mass spectra obtained at various cell pressures provided evidence for oligomeric ions as large as the pentameric species consisting of five directly linked carborane cages. It may be possible to produce larger oligomers at higher cell pressures.

Further experimental investigation will assist in determining the structures of these species. Ion/molecule reactions of the three carborane isomers, *o*-, *m*-, and *p*-$C_2B_{10}H_{12}$, will be compared with each other, and ion/molecule reactions involving carborane derivatives will be compared with the results obtained for underivatised carboranes. Fragmentation threshold studies could provide information about the strength of bonding between two directly linked carborane cages.

Mass spectra obtained in this study provided evidence for hydrogen loss and transfer in addition to the formation of H_2O/CH_3OH adduct ions. This resulted in very complex mass spectra containing many overlapped isotopic distributions. The interactive fitting program MACLOOMIS was adapted to mass spectra and greatly simplified the analysis of the spectra obtained, enabling the development of a simple reaction mechanism to describe the ion/molecule reactions of the complex *o*-$C_2B_{10}H_{12}$ system.

The MACLOOMIS approach, which utilises pattern recognition techniques to unravel overlapped isotopic distributions, will prove extremely useful in a wide range of high resolution mass spectrometry studies.

Acknowledgements

The authors gratefully acknowledge the help of Sally Duck, Department of Chemistry, Monash University, for maintaining and providing access to the FTICR mass spectrometer.

References

[1] J.L. Beauchamp, L.R. Anders, J.D. Baldeschwieler, J. Am. Chem. Soc. 89 (1967) 4569.
[2] J.S. Brodbelt, Mass Spectrom. Rev. 16 (1997) 91.
[3] N.M.M. Nibbering, Trends Anal. Chem. 13 (1994) 223.
[4] N.M.M. Nibbering, Acc. Chem. Res. 23 (1990) 279.
[5] J. Plesek, Chem. Rev. 92 (1992) 269.
[6] V.I. Bregadze, Chem. Rev. 92 (1992) 209.
[7] T.L. Heying, J.W. Ager Jr., S.L. Clark, D.J. Mangold, H.L.

Goldstein, M. Hillman, R.J. Polak, J.W. Szymanski, Inorg. Chem. 2 (1963) 1089.
[8] M.M. Fein, J. Bobinski, N. Mayes, N. Schwartz, M.S. Cohen, Inorg. Chem. 2 (1963) 1111.
[9] L.I. Zakharkin, V.I. Stanko, V.A. Brattstev, Yu.A. Chapovskii, Yu.T. Struchkov, Inz. Akad. Nauk SSSR, Ser. Khim. (1963) 2069.
[10] L.I. Zakharkin, V.I. Stanko, V.A. Brattstev, Yu.A. Chapovskii, O.Yu. Okhlobystin, Inz. Akad. Nauk SSSR, Ser. Khim. (1963) 2238.
[11] J.A. Dupont, M.F. Hawthorne, J. Am. Chem. Soc. 86 (1964) 1643.
[12] X. Yang, W. Jiang, C.B. Knobler, M.F. Hawthorne, J. Am. Chem. Soc. 114 (1992) 9719.
[13] J. Müller, K. Baše, T.F. Magnera, J. Michl, J. Am. Chem. Soc. 114 (1992) 9721.
[14] X.G. Yang, W. Jiang, C.B. Knobler, M.D. Mortimer, M.F. Hawthorne, Inorg. Chim. Acta 240 (1995) 371.
[15] Z. Janoušek, S. Hermánek, J. Plešec, B. Stíbr, Collect. Czech. Chem. Commun. 39 (1974) 2363.
[16] N.I. Kirillova, A.I. Klimova, Yu.T. Struchkov, V.I. Stanko, Zh. Struct. Khim. 17 (1976) 675.
[17] M.A. Mathur, T.J. Klingen, J. Inorg. Nucl. Chem. 38 (1976) 1597.
[18] R.H. Cragg, A.F. Weston, J. Organomet. Chem. 67 (1974) 161.
[19] N.I. Vasyukova, Yu.S. Nekrasov, Yu.N. Sukharev, V.A. Mazunov, Yu.L. Sergeev, Inz. Akad. Nauk SSSR, Ser. Khim. (1985) 1337.
[20] Yu.S. Nekrasov, D.V. Zverev, N.I. Vasyukova, A.I. Belokon, Inz. Akad. Nauk SSSR, Ser. Khim. (1995) 484.
[21] N.I. Vasyukova, Yu.S. Nekrasov, V.Ts. Kampel, V.I. Bregadze, Inz. Akad. Nauk SSSR, Ser. Khim. (1987) 567.
[22] T. Onak, J. Howard, C. Brown, J. Chem. Soc., Dalton Trans. (1973) 76.
[23] C.L. Brown, K.P. Gross, T. Onak, J. Am. Chem. Soc. 94 (1972) 8055.
[24] D. McNaughton, D. McGilvery, F. Shanks, J. Mol. Spectrosc. 149 (1991) 458.
[25] B.P. Winnewisser, J. Reinstädtler, K.M.T. Yamada, J. Behrend, J. Mol. Spectrosc. 136 (1989) 12.
[26] F.W. Loomis, R.W. Wood, Phys. Rev. 32 (1928) 223.
[27] G.H. Kruppa, P. Caravatti, C. Radloff, S. Zürcher, F. Laukien, C. Watson and J. Wronka, FT-ICR/MS: Analytical Applications of Fourier Transform Ion Cyclotron Resonance Mass Spectrometry, B. Asamoto (Ed.), Chap. 4, VCH, New York, 1991.
[28] B.B. Reinhold, V.N. Reinhold, J. Am. Soc. Mass. Spectrom. 3 (1992) 207.
[29] M.W. Senko, S.C. Beu, F.W. McLafferty, J. Am. Soc. Mass. Spectrom. 6 (1995) 52.
[30] Z.Z. Zhang, A.G. Marshall, J. Am. Soc. Mass. Spectrom. 9 (1998) 225.
[31] M. Whitbeck, Tetrahedron Comput. Methodol. 3 (1992) 497.